

Lab # 3 - Appendix A

Description of the Servo Module

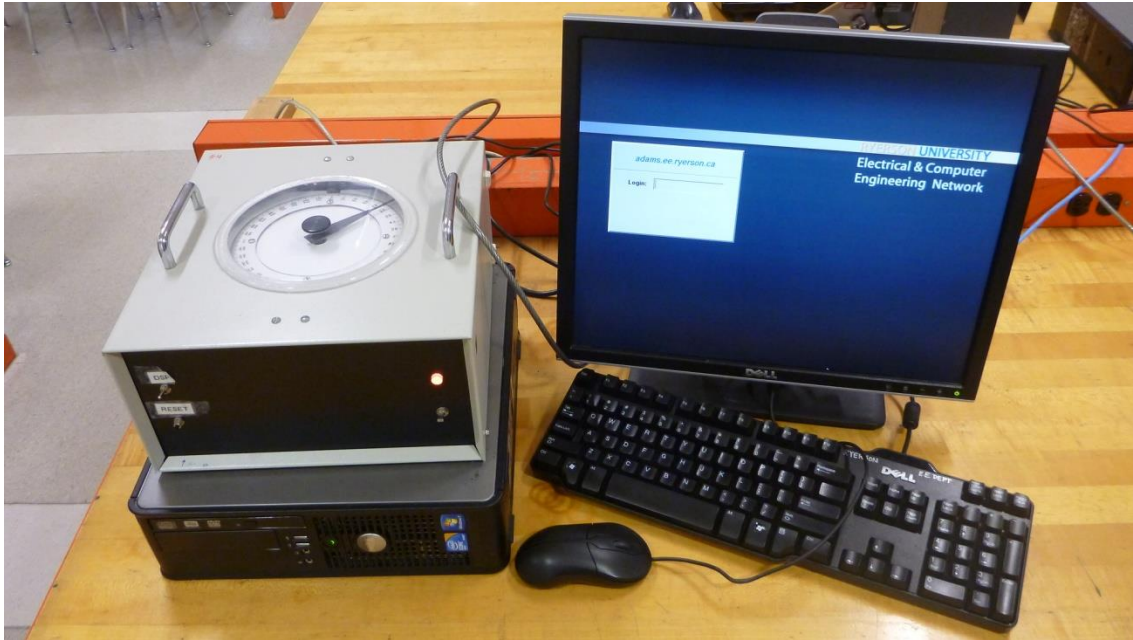


Figure 1: Experimental Setup in the Control Systems Lab

The objective of this lab experiment is to introduce you to operation and control of real-time control systems - Servo Modules in ENG413 Lab, and to a realistic model of these systems, i.e. one that includes various real-life non-linearities. To explain - the Servo Module is a rotational positioning system, and like all real-life systems, it is essentially non-linear, displaying such nonlinear characteristics as: the so-called dead-zone, gear backlash (also called “gearlash”), static friction and saturation.

Servo positioning systems are used to perform various tasks in which tracking a certain trajectory is required, such as articulation of a robot arm, automated assembly, such as spot-welding, or positioning tooling tables, positioning radar and satellite dishes, etc. In all cases either rotational or translational motion along one, two or even three axes is necessary. Articulators in servo systems are high precision DC motors. If necessary, their rotational motion can be translated into translational motion through a use of a rack and pinion or lead-screw mechanisms. The motion control, i.e. control of the system dynamics as well as computing an appropriate input trajectory for the system, is typically performed by a computer.

The Servo Module currently used in ELE639 Lab is shown in Figure 1. It contains a high precision geared DC motor, an optical encoder for reading the position of the motor shaft, a

power amplifier and a Motorola digital signal processing board with 16 bit D/A and A/D converters. A schematic diagram of the Servo is shown in Figure 2.

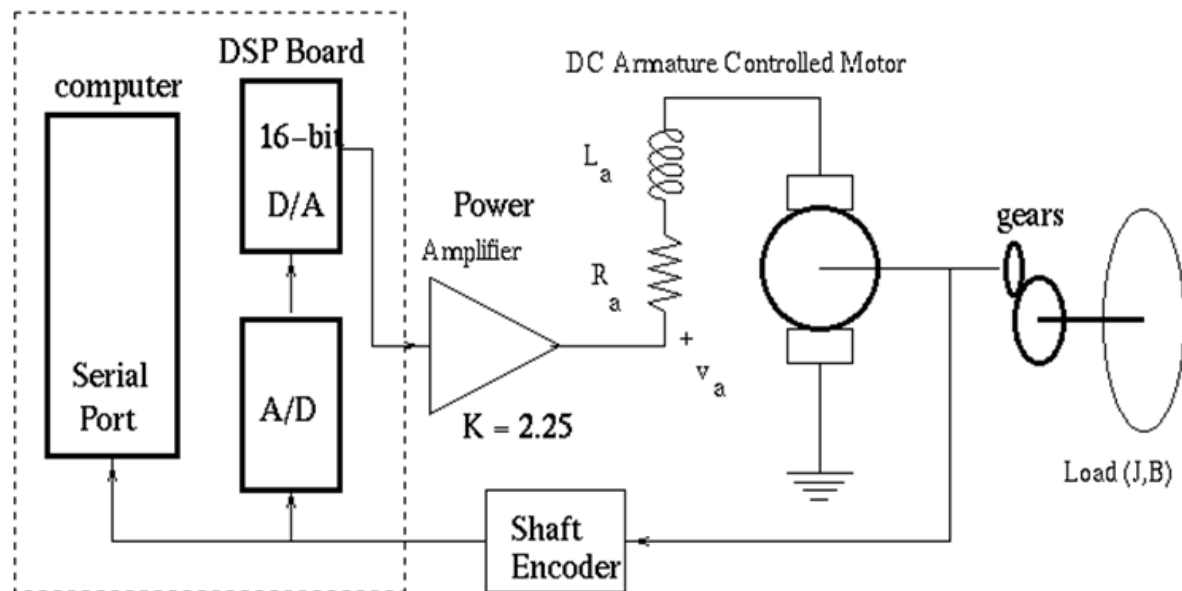


Figure 2: Schematic Diagram of the Servo Module

DC motors are common actuators in many control systems. They directly provide rotary motion and, when coupled with wheels or a rack-and-pinion mechanism, can provide translational motion. The picture to the left in Figure 3 shows an example of a large, high-powered industrial DC motor. The motor in our Servo Module is a small, light-weight, high-precision, armature-controlled DC motor, similar to the one shown in the picture to the right of Figure 3.

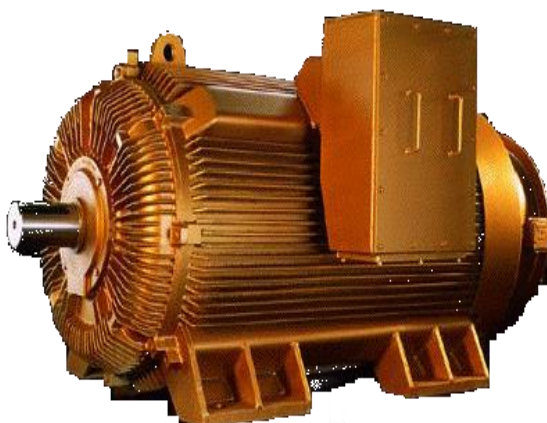


Figure 3: Examples of DC Motors (High Powered and Low Powered)

Small DC motors, such as the one in the lab, work most efficiently at high speeds, so in order to be used in a positioning system they have to be geared down, while direct drives are found in some industrial DC motors with large ratings. In robotic applications you're more likely to see a small, lightweight, high-precision geared DC motor, like the one shown on the right of Figure 3; however, regardless of whether a DC motor is large or small, its system equations follow the same laws of physics, allowing us to derive a general transfer function representation of it.

The DSP board shown in Figure 2 serves as an interface between the computer and the analog process, which consists of the DC motor, its load (i.e. the pointer) and an amplifier. The control of the angular position of the DC motor shaft is implemented using a menu-driven interface - see Appendix B for more detailed information on the Servo Module interface. The sampling rate used in data acquisition is high enough to ignore the digital nature of the system for the purpose of this analog control course.

Linear Model of the Servo Module

We shall first discuss the system description in its *linear* operating range, where the aforementioned real-life non-linearities can be reasonably ignored. A block diagram of the Servo Positioning Module is shown in Figure 4. The controlled output is the actual angular position of the motor shaft on the load side of the gear $\theta_L(t)$. The load is a pointer in the Servo casing, indicating the shaft position. The input to the system is the desired (reference) angular position of the motor shaft $\theta_{ref}(t)$. The output of the DSP board D/A converter is too low to drive the DC motor directly, and so a power amplifier is used in the setup, together with the motor.

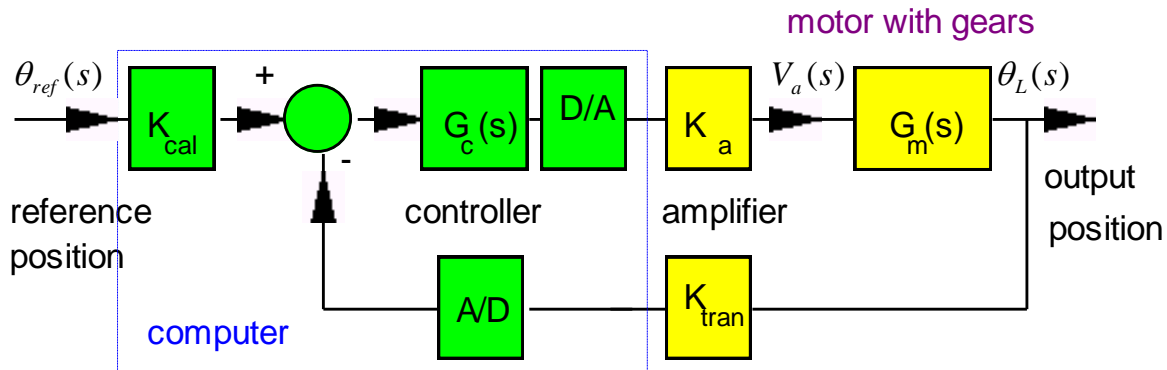


Figure 4: Block Diagram of a Linear Model of the Servo Module

Using the block diagram algebra rules, the input command calibration gain, K_{cal} , gains of D/A and A/D converters, as well as the optical shaft encoder gain, K_{tran} , can be eliminated. The block diagram of our system can be represented by an equivalent unit feedback system as shown in Figure 5. Next, a transfer function of the motor, $G_m(s)$, will be derived.

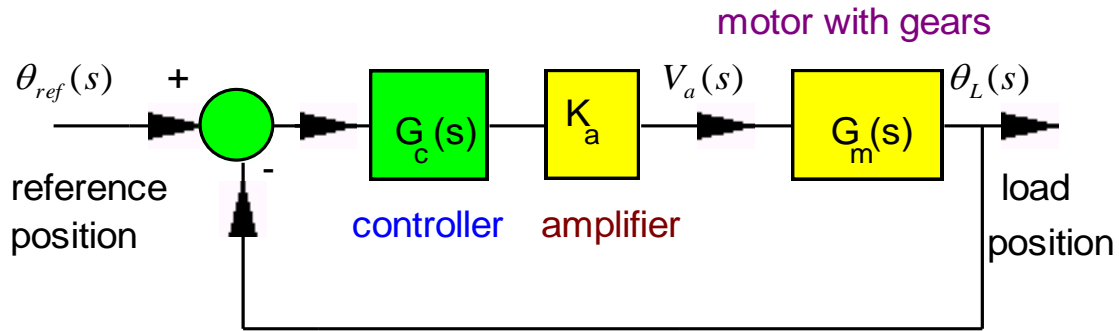


Figure 5: Unit-feedback Equivalent Block Diagram of the Servo Module

The diagram in Figure 6 is a representation of such DC armature-controlled motor, showing the electric circuit of the armature as well as mechanical parts of the motor, including gears.

DC Armature Controlled Motor

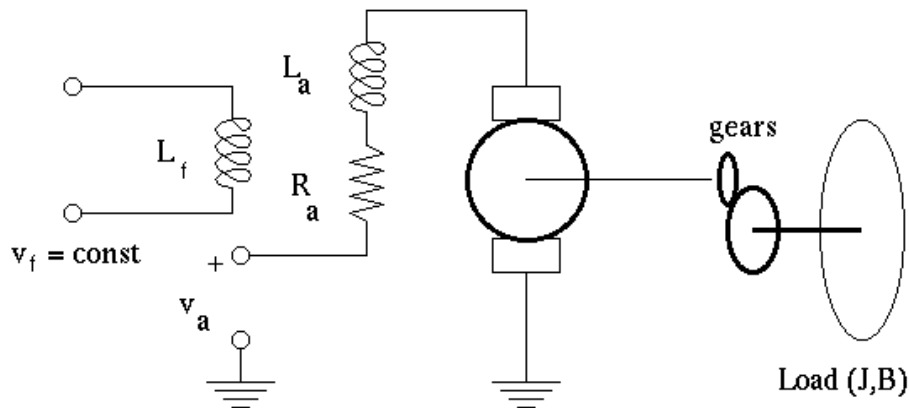
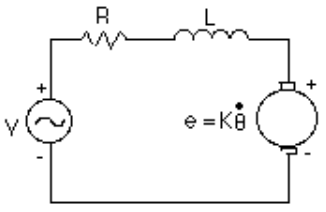
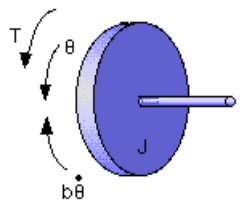
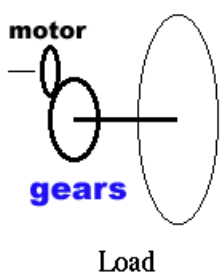


Figure 6: Schematic Diagram of an Armature Controlled DC Motor

Motor equations are shown in Table 1, where R and L represent the resistance and inductance of the armature winding, K_t and K_e represent the torque constant and the counter-electromotive force (CEMF) constant, respectively; n is the gear ratio and J_{eq} and B_{eq} represent respectively the equivalent inertia and viscous friction coefficients of the motor and load combined, as reflected onto the motor side of the gear.

Table 1: Basic Equations for the DC Motor

	<p>Armature winding:</p> $v_a - v_e = Ri + L \frac{di}{dt}$ <p>counter-electromotive (CEMF) force:</p> $v_e = K_e \omega$
	<p>Energy conversion: $T = K_t i$</p> <p>Mechanical part:</p> $J_{eq} \dot{\omega}_m = T - B_{eq} \omega_m$ $\omega = \dot{\theta}$
	$P_{motor} = P_{load}$ $T_m \omega_m = T_L \omega_L$ <p>gear ratio:</p> $\frac{T_m}{T_L} = \frac{\omega_L}{\omega_m} = \frac{1}{n}$ $J_m \dot{\omega}_m + (J_L \dot{\omega}_L) \cdot \frac{1}{n} = T - B_m \omega_m - (B_L \omega_L) \cdot \frac{1}{n}$ $J_{eq} = J_m + \frac{J_L}{n^2}$ $B_{eq} = B_m + \frac{B_L}{n^2}$

DC motor transfer function $G_m(s) = \frac{\Omega(s)}{V_a(s)}$, is defined as the dynamic ratio of the load position output signal and the armature voltage input signal. Based on the equations from Table 1, this transfer function can be represented by a block diagram shown in Figure 7, where the motor input is the armature voltage $\Omega(s)$, and the motor output is the shaft angular position $V_a(s)$.

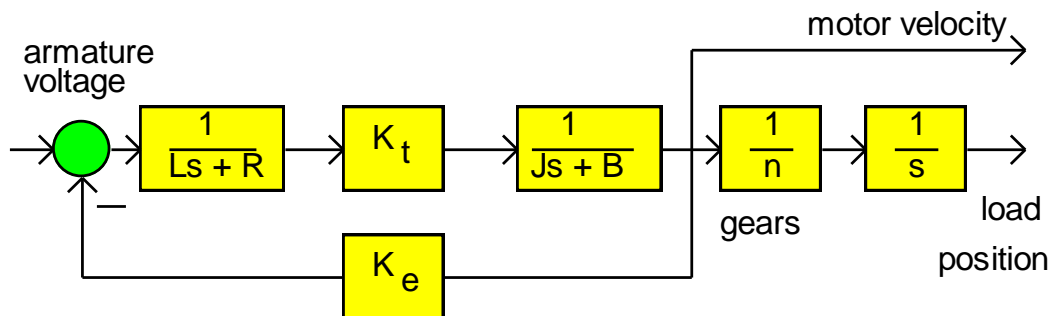


Figure7: Block Diagram of the DC Motor

Transfer function $G_m(s)$ can then be derived from the block diagram in Figure 7, as shown below:

$$G_m(s) = \frac{\frac{K_t}{(sL + R)(sJ_{eq} + B_{eq})}}{1 + \frac{K_t K_e}{(sL + R)(sJ_{eq} + B_{eq})}} \cdot \frac{1}{n} \cdot \frac{1}{s} = \frac{K_t}{s^2 L J_{eq} + s(RJ_{eq} + LB_{eq}) + RB_{eq} + K_t K_e} \cdot \frac{1}{n} \cdot \frac{1}{s}$$

Going back to Figure 4, assuming that the system works under Proportional Control with gain K_p , the open and closed loop transfer functions of the linearized model of the Servo Module can now be derived:

$$G_{open}(s) = G_c(s) \cdot K_a \cdot G_m(s) = K_p \cdot K_a \cdot \frac{K_t}{s^2 L J_{eq} + s(RJ_{eq} + LB_{eq}) + RB_{eq} + K_t K_e} \cdot \frac{1}{n} \cdot \frac{1}{s}$$

$$G_{closed}(s) = \frac{G_{open}(s)}{1 + G_{open}(s)} = \frac{K_p K_a \frac{K_t}{s^2 L J_{eq} + s(RJ_{eq} + LB_{eq}) + RB_{eq} + K_t K_e} \cdot \frac{1}{n} \cdot \frac{1}{s}}{1 + K_p K_a \frac{K_t}{s^2 L J_{eq} + s(RJ_{eq} + LB_{eq}) + RB_{eq} + K_t K_e} \cdot \frac{1}{n} \cdot \frac{1}{s}}$$

$$G_{closed}(s) = \frac{K_p K_a K_t}{(s^2 L J_{eq} + s(RJ_{eq} + LB_{eq}) + RB_{eq} + K_t K_e)n \cdot s + K_p K_a K_t}$$

$$G_{closed}(s) = \frac{K_p \cdot K_a \cdot K_t}{L J_{eq} n \cdot s^3 + (R J_{eq} + L B_{eq}) n \cdot s^2 + (R B_{eq} + K_t K_e) n \cdot s + K_p K_a K_t}$$

The closed loop system is thus described by a 3rd order transfer function, with no zeros and three poles. Note that the transfer function of the motor, $G_m(s)$, was also of 3rd order - the additional components of the control system (i.e. the controller, the amplifier and transducers) are assumed to have no dynamics and are represented by straight gains.

Now, recall the concept of a simplified model for a physical system, based on dominant system dynamics. In many motors, inductances L are small, so that $L/R \ll J/B$. This means that out of the two motor time constants (i.e. electrical and mechanical), the electrical one, which is a ratio of inductance over resistance ($\tau_{electr} = \frac{L}{R}$), is much smaller than the mechanical one, which is a ratio of inertia over friction ($\tau_{mech} = \frac{J}{B}$). The motor dynamics can thus be simplified, by ignoring the contributions of the electrical time constant, to a 2nd order model, described by this transfer function:

$$G_m(s) \approx \frac{K_t}{sRJ_{eq} + RB_{eq} + K_t K_e} \cdot \frac{1}{n} \cdot \frac{1}{s}$$

The motor transfer function $G_m(s)$ can therefore be written, in its simplified version, as:

$$G_m(s) = \frac{K_m}{s\tau_m + 1} \cdot \frac{1}{n} \cdot \frac{1}{s}$$

where K_m is called the *motor gain constant*, and τ_m is called the *motor time constant*:

$$K_m = \frac{K_t}{RB + K_t K_e} \quad \tau_m = \frac{RJ}{RB + K_t K_e}$$

$G_m(s)$ can now be represented by a block diagram in Figure 8:

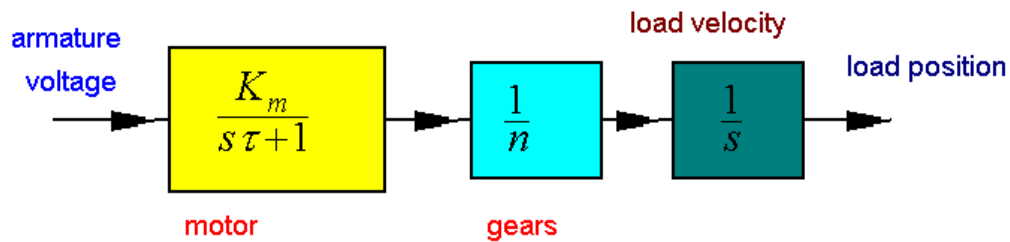


Figure 8: Block Diagram of the Simplified Model of DC Motor

The simplified model of $G_m(s)$ is of second order, and in this case, the closed loop transfer function would also be of the second order, as follows.

$$G_{open}(s) = G_c(s) \cdot K_a \cdot G_m(s) = K_p \cdot K_a \cdot \frac{K_m}{s\tau_m + 1} \cdot \frac{1}{n} \cdot \frac{1}{s}$$

$$G_{closed}(s) = \frac{G_{open}(s)}{1 + G_{open}(s)} = \frac{K_p K_a \cdot \frac{K_m}{s\tau_m + 1} \cdot \frac{1}{n} \cdot \frac{1}{s}}{1 + K_p K_a \frac{K_m}{s\tau_m + 1} \cdot \frac{1}{n} \cdot \frac{1}{s}}$$

$$G_{closed}(s) = \frac{K_p K_a K_m}{(s\tau_m + 1)n \cdot s + K_p K_a K_t}$$

$$G_{closed}(s) = \frac{K_p \cdot K_a \cdot K_m}{\tau_m n \cdot s^2 + n \cdot s + K_p K_a K_m}$$

How accurate is this approximation? Figure 9 shows closed loop responses of the accurate servo module model and the model using a 2nd order approximation for the DC motor - the responses are practically identical.

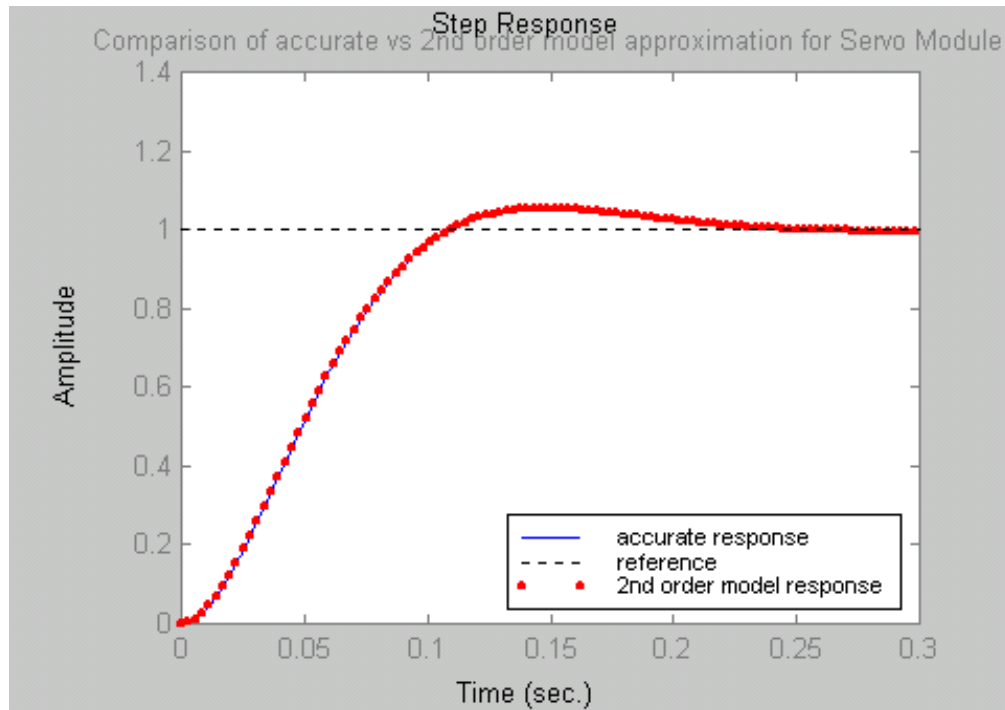


Figure 9: Responses of the Servo Module and its 2nd Order Approximate Model

Numerical value of the motor transfer function can be calculated based on **nominal** parameter values provided by hardware manufacturers. These often contain different unit sets, such as imperial units - all such units have to be converted into the SI system. Some of the system parameters are not available directly and have to be calculated.

Below is a list of parameter values as provided by the manufacturer of DC motors in the Servo Modules in ENG413 Lab:

1. $L = 0.15mH$ - armature inductance
2. $R = 3\Omega$ - armature resistance
3. $K_t = 0.863 \frac{oz \cdot in}{A}$ - torque constant
4. $K_e = 0.639 \cdot 10^{-3} \frac{V \cdot min}{rev}$ - CEMF force constant
5. $B_L \approx 0 \text{ N} \cdot m \cdot sec$ - viscous friction of the load is assumed negligible
6. Motor to load shaft gear ratio is **1** to **17.2**
7. $T_{nl} = 0.017 oz \cdot in$ - no-load resistance torque; $\omega_{nl} = 9300 rpm$ - no-load motor speed
8. Servo Amplifier Gain:

$$K_a = 2.25V/V \text{ - for Motors 3, 6, 8, 9, 10, 11}$$

$$K_a = 1.0V/V \text{ - for Motors 1, 2, 4, 5, 7}$$

Since the motor is geared, equivalent values of J and B coefficients have to be calculated, as reflected onto the motor side of the shaft. Let us first calculate the equivalent inertia coefficient of the motor J_{eq} , as described in Table 1. From the manufacturer data we have:

$$J_m = 0.35 \cdot 10^{-4} oz \cdot in \cdot sec^2 \text{ - inertia of the motor}$$

$$J_L = 2 \cdot 10^{-5} N \cdot m \cdot sec^2 \text{ - inertia of the load (the pointer in the Servo casing)}$$

$$\frac{1}{n} = \frac{1}{17.2}$$

$$J_m = 0.35 \cdot 10^{-4} oz \cdot in \cdot sec^2 = 2.471 \cdot 10^{-7} N \cdot m \cdot sec^2$$

$$J_{eq} = J_m + \frac{J_L}{n^2} = 3.147 \cdot 10^{-7} N \cdot m \cdot sec^2$$

NOTE:

$$J_m = 2.5 \cdot 10^{-7} N \cdot m \cdot sec^2 \text{ describes Lab Servos 1 to 9; Servomotor 10 has a different inertia:}$$

$$J_m = 6.5 \cdot 10^{-7} N \cdot m \cdot sec^2$$

Next, the viscous friction coefficient B_{eq} needs to be calculated, as described in Table 1. The viscous friction coefficient for the motor, B_m , is not available, but can be calculated from the no-load values of torque and speed:

$$B_m = \frac{T_{nl}}{\omega_{nl}}$$

From the manufacturer data we have:

$$B_m = \frac{T_{nl}}{\omega_{nl}} = \frac{0.017 \text{ oz} \cdot \text{in}}{9300 \text{ r.p.m.}} = 1.233 \cdot 10^{-7} \text{ N} \cdot \text{m} \cdot \text{sec}$$

Note that the viscous friction of the load is assumed negligible: $B_L \approx 0 \text{ N} \cdot \text{m} \cdot \text{sec}$. Next, we can compute the equivalent friction coefficient.

$$B_{eq} = B_m + \frac{B_L}{n^2} \approx B_m = 1.233 \cdot 10^{-7} \text{ N} \cdot \text{m} \cdot \text{sec}$$

We are ready to calculate the motor gain constant K_m . Note that radian is a non-dimensional unit. We can also calculate the motor time constant τ_m .

$$\begin{aligned} K_m &= \frac{K_t}{RB + K_t K_e} = \frac{6.094 \cdot 10^{-3} \text{ N} \cdot \text{m}}{\left(3\Omega \cdot 1.23 \cdot 10^{-7} \text{ N} \cdot \text{m} \cdot \text{sec} + 6.094 \cdot 10^{-3} \frac{\text{N} \cdot \text{m}}{\text{A}} \cdot 6.094 \cdot 10^{-3} \frac{\text{V} \cdot \text{sec}}{\text{rad}} \right) \cdot \text{A}} = \\ &= \frac{6.094 \cdot 10^{-3} \text{ N} \cdot \text{m}}{\left(3 \frac{\text{V}}{\text{A}} \cdot 1.23 \cdot 10^{-7} \text{ N} \cdot \text{m} \cdot \text{sec} + 6.094 \cdot 10^{-3} \frac{\text{N} \cdot \text{m}}{\text{A}} \cdot 6.094 \cdot 10^{-3} \frac{\text{V} \cdot \text{sec}}{1} \right) \cdot \text{A}} = \\ &= \frac{6.094 \cdot 10^{-3} \text{ N} \cdot \text{m}}{\left(3 \cdot 1.23 \cdot 10^{-7} + 6.094 \cdot 10^{-3} \cdot 6.094 \cdot 10^{-3} \right) \frac{\text{N} \cdot \text{m} \cdot \text{V} \cdot \text{sec}}{\text{A}}} = \\ &= 162.056 \frac{1}{\text{V} \cdot \text{sec}} = 162.056 \frac{\text{rad}}{\text{V} \cdot \text{sec}} \\ \tau_m &= \frac{RJ}{RB + K_t K_e} = \frac{3\Omega \cdot 3.147 \cdot 10^{-3} \text{ N} \cdot \text{m} \cdot \text{sec}^2}{\left(3\Omega \cdot 1.23 \cdot 10^{-7} \text{ N} \cdot \text{m} \cdot \text{sec} + 6.094 \cdot 10^{-3} \frac{\text{N} \cdot \text{m}}{\text{A}} \cdot 6.094 \cdot 10^{-3} \frac{\text{V} \cdot \text{sec}}{\text{rad}} \right)} = \\ &= \frac{3\Omega \cdot 3.147 \cdot 10^{-3} \text{ N} \cdot \text{m} \cdot \text{sec}^2}{\left(3 \cdot 1.23 \cdot 10^{-7} + 6.094 \cdot 10^{-3} \cdot 6.094 \cdot 10^{-3} \right) \frac{\text{N} \cdot \text{m} \cdot \text{V} \cdot \text{sec}}{\text{A}}} = \\ &= \frac{3 \cdot 3.147 \cdot 10^{-3} \cdot \Omega \cdot \text{N} \cdot \text{m} \cdot \text{sec}^2}{\left(3 \cdot 1.23 \cdot 10^{-7} + 6.094 \cdot 10^{-3} \cdot 6.094 \cdot 10^{-3} \right) \Omega \cdot \text{N} \cdot \text{m} \cdot \text{sec}} = 0.0251 \text{ sec} \end{aligned}$$

$$K_m = 162.056 \frac{1}{V \cdot \text{sec}} \quad \tau_m = 0.0251 \text{ sec}$$

Finally, we are ready to compute the motor transfer function as described by its approximate 2nd order model:

$$G_m(s) \approx \frac{K_m}{s\tau_m + 1} \cdot \frac{1}{n} \cdot \frac{1}{s} = \frac{162.056}{0.0251s + 1} \cdot \frac{1}{s} \cdot \frac{1}{17.2}$$

Thus derived transfer function $G_m(s)$ now describes the motor block in the linear model of the Servo setup, shown in Figure 4. Please check that the unit dimensions of the denominator of the first block of the transfer function cancel out, as the Laplace operator “s” has the dimension of frequency. The unit of frequency is rad/sec, and since radian has no dimensions, the dimension of “s” is 1/sec. Thus the overall dynamic gain of the motor K_m is described by the units of the motor gain constant divided by the unit of the “s” operator in the second, integrator term. Thus, the overall dimension of $G_m(s)$ is shown as:

$$s = \sigma + j\omega$$

$$[G_m(s)] = \frac{1}{V \cdot \text{sec}} \cdot \frac{1}{\frac{1}{\text{sec}}} = \frac{1}{V}$$

Check this result against the definition of the motor transfer function, based on the block diagrams in Figure 7 and Figure 8. In these diagrams, the motor transfer function $G_m(s)$ is defined as the dynamic ratio of the load position output signal and the armature voltage input signal:

$$G_m(s) = \frac{\theta_L(s)}{V_A(s)}$$

The load position unit is rad/sec, and the armature voltage unit is Volt. Thus, the dimension of $G_m(s)$ is the same calculated both ways. This is a check on the correctness of our derivation procedure. The system parameters are derived in SI units, where the unit for angular position is radian. However, we are all much more comfortable with the angular position expressed in degrees, and thus the Servo is calibrated in degrees.

Non-Linear Model of the Servo Module

All real life systems display some non-linear behaviours. Sometimes nonlinearities do not affect the system behaviour within an operating range and the LTI model can be safely assumed. In other cases non-linearities cannot be ignored. Nonlinearities in the Servo Module are associated with:

- Sampling and quantization error
- DC offset in the D/A output
- Saturation of the controller output
- Backlash in gears (“gearlash”) and static friction (stiction) – resulting in the so-called “dead-zone” behaviour.

The first two are negligible in the Servo Module, but the latter two affect the system response in a significant manner. A full analytical treatment of the system nonlinearities is outside of the scope of this course. In the Servo Module, saturation is caused by a limited linear range of the D/A converter in the DSP board. D/A output limits are specified by the DSP board manufacturer to be $\pm 1.4V$. An illustration of the saturation effect on the system response is shown in Figure 10, showing the Servo response to a 300° reference. This large input signal will cause the controller output to saturate.

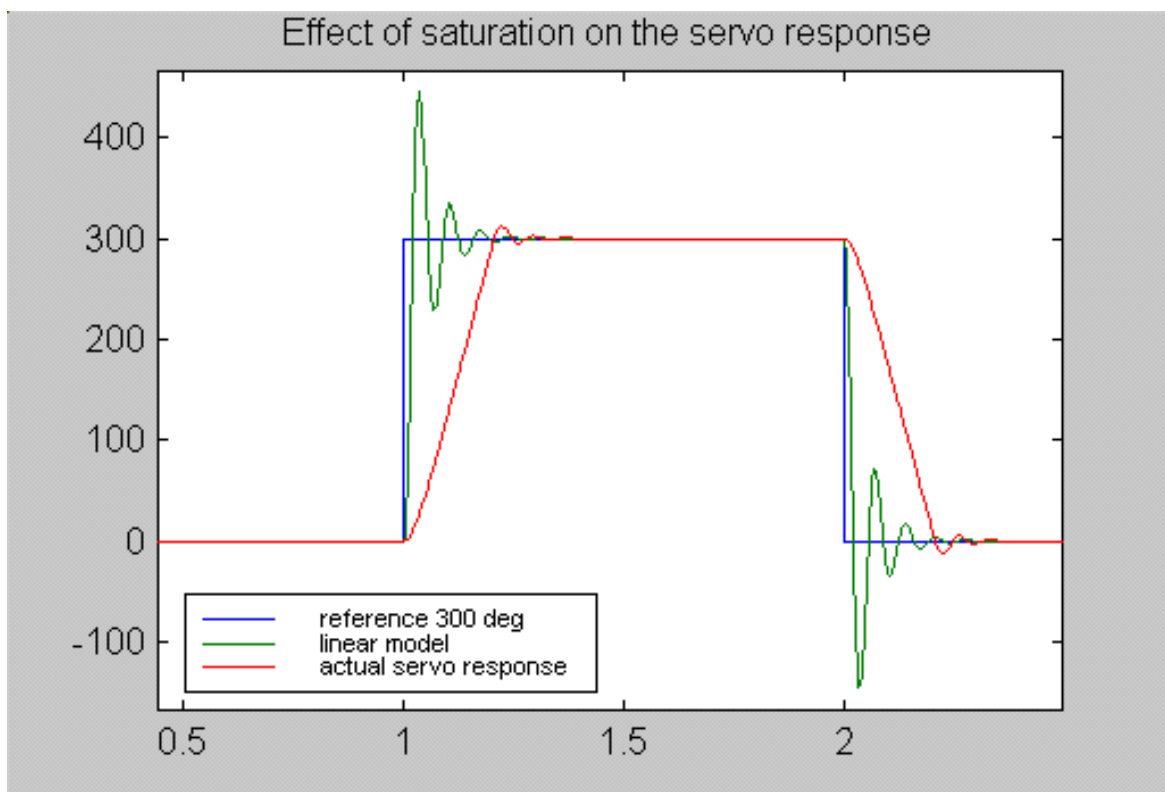


Figure 10: Saturation in the Servo Module

The **gear-lash** and **stiction** are the effects that are visible on the Servo Module response for low values of the input signal. As the signal switches polarity, its amplitude is small enough to clearly show that the system output keeps getting “stuck” in the so-called *Dead-zone*.

This is perhaps best illustrated by Figure 11, which shows the servo response to a small magnitude ramp input, with a very low value of the gain ($K = 0.5$). Notice that until $t = 1.35$ sec, the output of the system is still zero, i.e. the output signal is “stuck” in the Dead-zone.

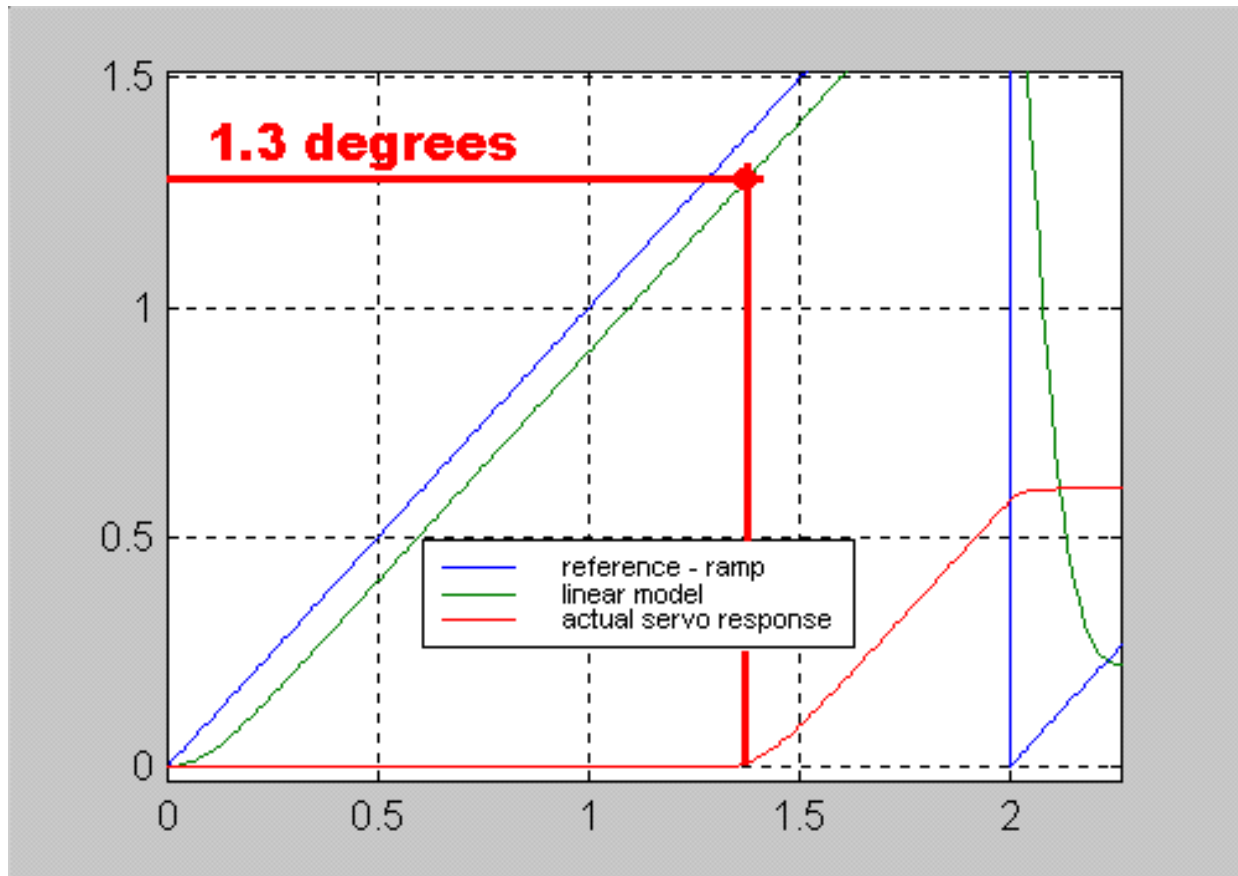


Figure 11: Measurement of the Dead-zone in the Servo Module

Figure 12 shows the Servo response to a small input reference of 20° , with a very visible effect of the Dead-zone. The system response does not have a zero steady state error, as expected from system of Type 1 – on the contrary, a large steady state error is visible. Notice the motor response is not symmetrical, indicating different values of the Dead-zone “threshold”, dependent on the signal polarity.

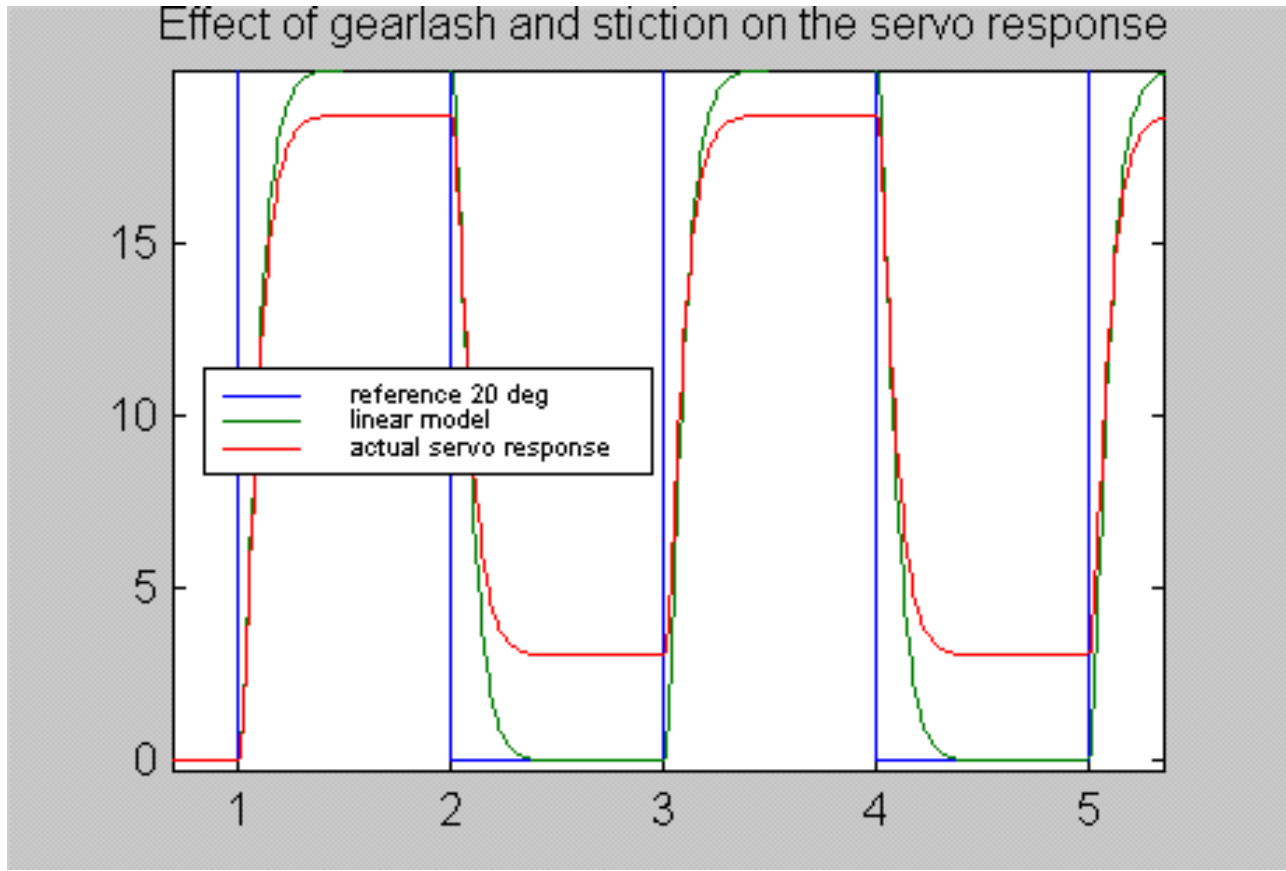


Figure 12: The Effect of Gear-lash and Stiction in the Servo Module – Dead-zone

There is no manufacturer data available on the Dead-zone, however, it can be estimated as follows. In Figure 11, at $t = 1.35 \text{ sec}$ the output of the system is still zero. Based on the block diagram, we can compute the level of the threshold signal d , using this formula:

$$d = A \frac{\pi}{180} K_c K_a$$

$A = 1.3^\circ$ is the magnitude of the input at $t = 1.35 \text{ sec}$ (in degrees), and K_c, K_a are controller and amplifier gains, respectively. The power amplifier gain used in the system is $K_a = 2.25 \text{ V/V}$. The Dead-zone threshold is thus calculated as $d = 0.008 \text{ V}$.

Nonlinearities of the type found in the Servo can be *simulated* using SIMULINK to obtain realistic results. Note that in this project you are **NOT** required to simulate the Servo model in Simulink, and the information that follows is **for your information only**, so that you can better understand the nature of the physical system, and the various ways it can be modeled.

Simulink has non-linear simulation blocks both for the Saturation effect and for the Dead-zone effect. The closed loop servo block diagram including nonlinear blocks is shown in Figure 13, and an example of Simulink simulation diagrams for this non-linear system is shown

in Figure 14. Saturation occurs at the output of the controller - the second part of Figure 14 diagram.

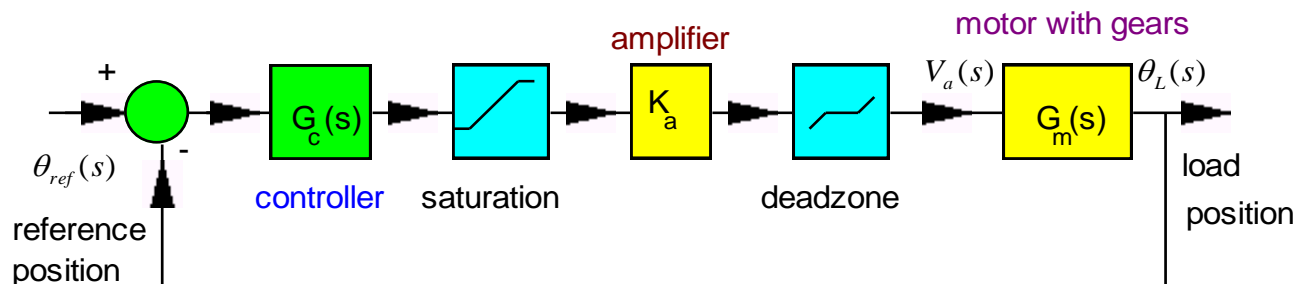


Figure 13: Block Diagram of the Servo Module with Nonlinearities

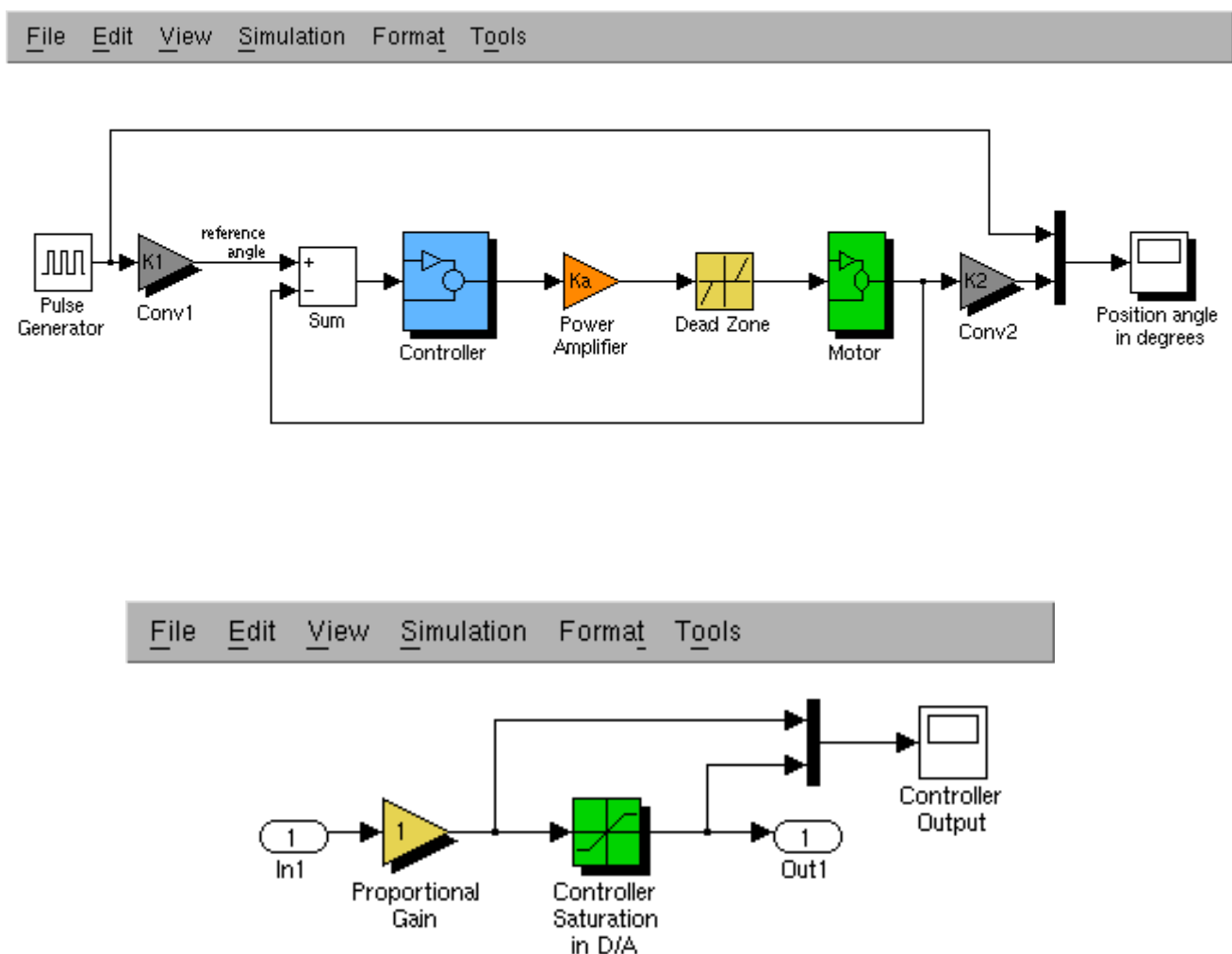


Figure 14: Simulink Diagrams for a nonlinear Model of the Servo